Journal of
Materials Chemistry A

Accepted Manuscript

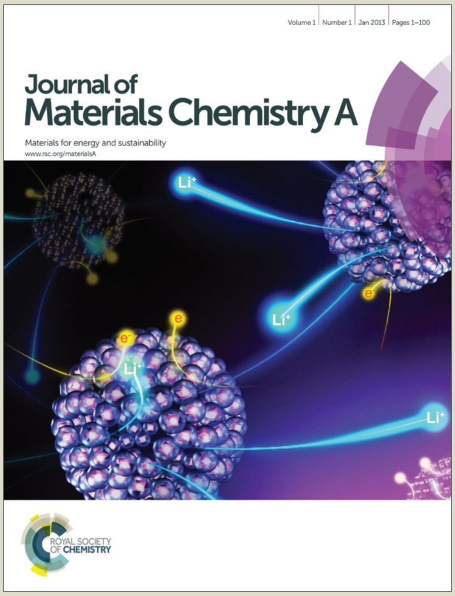

ROYAL SOCIETY
OF CHEMISTRY

www.rsc.org/materialsA

Journal of Materials Chemistry A

Journal of Materials Chemistry A

Dynamic Article Links ▶

PAPER

Cite this: DOI: 10.1039/c0xx00000x

www.rsc.org/xxxxxx

Highly Stable Poly(ethylene glycol)-Grafting Alkaline Anion Exchange Membranes

Congrong Yang,[a,b] Suli Wang,[a] Wenjia Ma,[a] Shixiong Zhao[a] Ziqi Xu[c] and Gongquan Sun[a,*]

Received (in XXX, XXX) XthXXXXXXXXX 20XX, Accepted Xth XXXXXXXXX 20XX

DOI: 10.1039/b000000x

A mechanically and chemically stable poly(ethylene glycol) (PEG)-grafting poly(styrene-ethylene-co-butylene-styrene) (SEBS)-based AAEMs was designed, prepared and characterized. The elongation at break of these SEBS-based AAEM was up to 500%, a value 80 times greater than that of AAEM using polystyrene as main chain. Remarkably, the IEC, conductivity， dimension and mechanical property of this AAEM could remain almost unchangeable in 2.5 M KOH at 60 °C for about 3000 h, indicating the excellent alkaline stability of the PEG-grafting SEBS-based AAEMs. Confirmed by TEM, the graft of PEG could enlarge the size of the ion-conducting channel, significantly enhancing the con-ductivity of these AAEMs (80 °C, from 29.2 mS cm^{-1} to 51.9 mS cm^{-1}). Furthermore, the peak power density of H_2/O_2 single fuel cell using this SEBS-based AAEM was up to 146 mW cm^{-2} at 50 °C. Based on the outstanding properties, this membrane is available for not only fuel cells but also other electrochemical energy conversion and storage devices, such as redoxflow and alkaline ion batteries.

Introduction

Favoring the use of non-precious metal catalysts, alka-line anion exchange membranes (AAEMs) have been evoked great interests in many electrochemical energy systems, such as fuel cells[1-3], flow[4, 5] and metal/air batteries[6], electrolyzers[7, 8], reverse electrodialysis cells[9] and bioelectrochemical systems[10]. For the above systems application, the AAEMs should possess good physical and chemical properties (not only high ionic conductivity and good mechanical strength but also high chemical stability). In the past decades, great efforts have been devoted to enhancing the performance of AAEMs for the requirement of the electrochemical systems. However, it is not easy to prepare an AAEM that could fulfill all the requirements. Two main disadvantages，relatively poor chemical stability and low ion conductivity (especially when the AAEM is not fully hydrated), of AAEM restrict its wide application. Up to date, the conductivity of the AAEM has been greatly improved (more than 0.1 Scm^{-1} at 80 °C) with the effort of the researchers[11, 12]. Therefore, in the severe alkaline environment, the chemical stability of AAEMs is still considered to be a primary and tough issue due to the presence of OH^-, a strong nucleophilic ion[13, 14]. Though the lifetime studies indicate that the cation stability is of paramount importance for stable operation of AAEMs[12, 15-29], equally important is the stability of the polyaromatic backbone under high pH conditions from the recent study results. It has been proved that the aromatic containing ether-based main chain would be severely degraded via the ether hydrolysis or (and) quaternary carbon hydrolysis in the alkaline solution at 60 °C[30, 31]. Therefore, a stable polymer main chain is also greatly important for the improvement of AAEMs.

According to our previous work, polystyrene main chain has been proved to possess better alkaline stability than that of poly(2,6-dimethyl-1,4-phenylene oxide)(PPO), polysulfone and other aromatic containing ether main chain, which is also found in other groups[28]. However, the poor mechanical stability (especially when AAEMs are in the dry condition) of AAEMs based on polystyrene (a rigid polymer) is a challenge for the application of this membrane.

In order to achieve a mechanically and chemically sta-ble AAEMs, poly(styrene-ethylene-co-butylene-styrene) (SEBS) with good flexility is selected as the main chain of AAEMs in this work. To further enhance the conductivities of the SEBS-based AAEMs, effective ion-conducting channel would be constructed in the AAEMs by grafting the PEG onto the SEBS main chain. The influences of the chloromethylation degree of SEBS and the graft state of PEG (molecular weight and graft degree) on the morphology and the physical and chemical properties (such as IEC, water uptake, swelling degree and ionic conductivity) are investigated in detail.

Experimental section

Materials

SEBS 6152 (molecular weight of 70000, styrene of 27%) is from Taipol company. 1,4-Bis(chloromethoxyl) butane (BCMB) is from Langene bio-science Co., Ltd.. Anhydrous tin chloride, poly(ethylene glycol) monomethyl ether (MPEG) (350, 750 and 1000), sodium hydride (60% w/w in mineral oil) and trimethylamine aqueous solution were purchased from Aladdin Industrial Inc.

Preparation of poly(ethylene glycol) grafted SEBS-based AAEMs

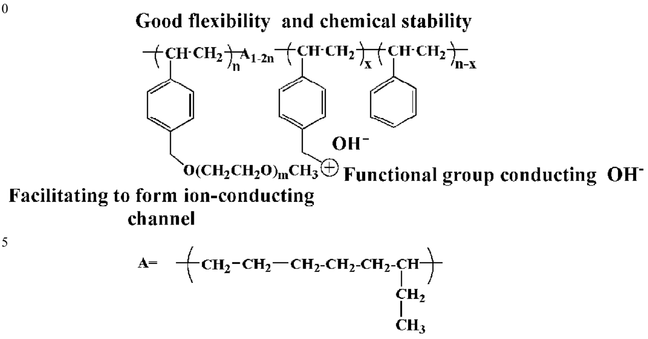

Fig. 1. Molecular structure of the designed polymer for the preparation of AAEMs.

To obtain a highly stable and conductive AAEM, the molecular structure of the polymer used for preparing AAEMs was designed as shown in Fig. 1. SEBS, the main chain, possesses good flexibility and good chemical stability in alkaline condition, which is suitable for AAEMs. The processes for the poly(ethylene glycol) grafted SEBS-based AAEMs include chloromethylation, PEG-grafting and quaternization. The synthetic routes were shown in Scheme 1. The chloromethylation of SEBS and PEG-grafting were considered to be two rather important processes that determined the properties of PEG-grafting SEBS-based AAEMs. Therefore, the influence of CD, PEG-grafting degree and the molecular weight of PEG on the microstructure and the properties of the AAEMs were investigated in detail.

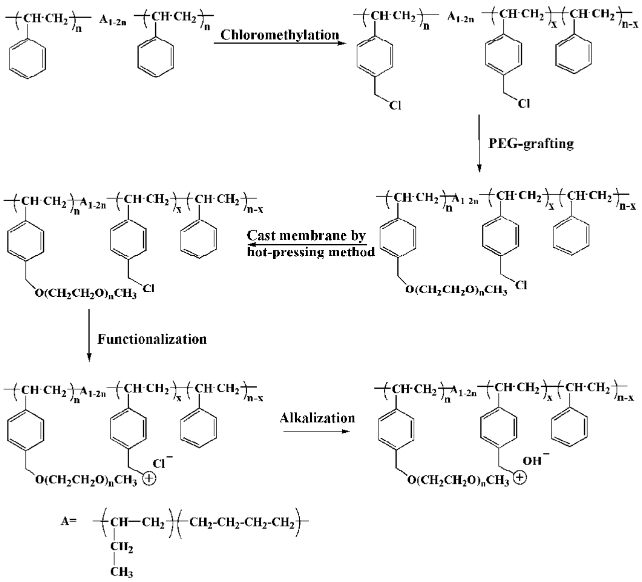

Scheme 1. Synthetic routes of poly(ethylene glycol)-grafting SEBS-based AAEMs.

Chloromethylation of SEBS

The chloromethylation of SEBS was achieved by the reaction of SEBS polymer and BCMB catalyzed by anhydrous tin chloride. The chloromethylation degree of SEBS could be effectively modulated by controlling the reaction temperature and reaction time. The reaction is as follows: SEBS (2g) was dissolved in CCl4 (30 mL) at 40 ^oC. Anhydrous tin chloride (0.5 mL) was added into the solution at 5 ^oC, followed by the drop addition of BCMB (3 mL). The mixture was stirred below 20 ^oC for a period of time and poured into ethanol to precipitate the product. The crude product was dissolved in THF and then precipitated again by ethanol. After being washed with ethanol and water for several times, the product was dried under vacuum condition at room temperature.

Preparation of PEG-grafted SEBS-based membranes

The grafting of PEG onto SEBS main chain was by the reaction of SEBS chloride and poly(ethylene glycol) monomethyl ether (MPEG). The above synthesized SEBS chloride was dissolved in THF (3% w/v). A certain amount of MPEG was added into the solution and the NaH was slowly added. The mixture reacted at 40 ^oC for 14 h. Then it was pour into ethanol, obtaining the light yellow and little transparent solid. The product was dried under vacuum condition at 30 ^oC. Finally, the PEG-grafted SEBS-based membranes were prepared by hot-pressed method with 20000 pounds pressure at 120 ^oC.

Quaternization of PEG-grafting SEBS-based membranes

The above prepared membranes were quaternized by immersing them in the trimethylamine aqueous solution at room temperature for 24 h. The membranes could be changed into OH^- form via treating the membranes in Cl^- form in 1 M KOH solution at room temperature for two days. The membranes were defined as QA-$SEBS_x$-g-PEG_y-M (QA is quaternary ammoniums, x is chloromethylation degree (CD), y is PEG-grafting degree and M is the molecular weight of MPEG).

NMR spectra

^1H NMR spectra were carried out on Bruker ACIII 400 spectrometer. CD of SEBS and PEG-grafting degree (x and y) could be calculated by the relative integrated intensities of the 1H resonances, respectively (as shown in Fig. S1, CDCl3 as solvent).

Morphological characterization

The morphologies of the membranes were characterized by transmission electron microscopy (TEM) using JEM-2100 with 200 kV. TEM sections were prepared using an ultracryomicrotome. For observation, these samples were stained by exposure to H_2PtCl6 (in ethylene glycol). The TEM data represent partially hydrated films that have been equilibrated under ambient conditions.

Ionic conductivity of the membranes

The resistance values of the AAEMs were measured over the frequency range from 1 Hz to 1 MHz by alternating current (ac) impedance spectroscopy using an electrode system connected with Solartron 1287 electrochemical workstation and Solartron 1260 gain-phase analyzer. All samples were placed in deionized water and equilibrated for at least 30 min at a given temperature. The membranes were repeatedly conducted for three times.

The in-plane conductivity was calculated as follows:

$$\sigma = \frac{L}{WTR}$$

where σ is the conductivity of the membrane in S cm^{-1}, L is the length of the membrane between sensor II and reference electrodes in cm, W and T are the width and thickness of the membrane in cm, respectively. R is the resistance of the membrane in ohm.

Ion exchange capacity (IEC), water uptake (WU), swelling degree (SD) and absorbed water capacity (λ) of the membranes

IEC of the AAEMs was determined by the back-titration method. The AAEMs in OH- form were immersed in 10 mL 0.01 $molL^{-1}$ HCl solution for two days. Then the solutions were titrated with the 0.01 M KOH solution using pH meter to determine the titration-end point. IEC values were calculated using the following expression:

$$IEC(mmol\,g^{-1}) = \frac{V_{0KOH}C_{KOH} - V_{iKOH}C_{KOH}}{m_{dry}} \times 1000$$

where V_{oKOH} and V_{iKOH} are the volumes of the KOH consumed in the titration without and with membranes, respectively, C_{KOH} was the molar concentration of KOH, and m_{dry} is the mass of the dried membrane in OH^- form.

The WU and the SD of the membranes in OH^- form are calculated from the weight and dimension differences of membranes after soaking in deionized water for 48 h at room temperature and after drying in a vacuum oven at 60 °C.

The WU is calculated by the equation as follows:

$$WU(\%) = \frac{W_{wet} - W_{dry}}{W_{dry}} \times 100$$

where W_{wet} and W_{dry} are the weight of wet and dry membranes in OH^- forms in grams, respectively.

The SD was calculated by the equation as follows:

$$SD(\%) = \frac{L_{wet} - L_{dry}}{L_{dry}} \times 100$$

where L_{wet} and L_{dry} are the geometric width of the wet and dry membranes in OH^- forms, respectively.

The number of absorbed water molecules per functional group, λ, was calculated as the following equation:

$$\lambda = \frac{WU}{M_{H_2O} \times IEC} \times 10$$

Thermomechanical stability of AAEMs

The thermomechanical performances of the grafted SEBS-based AAEMs were tested by DMA using a Q800 dynamic mechanical analyzer from TA Instruments in the stretching mode. The samples were heated from 100 to 300 °C at a heating rate of 3 °C min^{-1} under dry air atmosphere. A frequency of 1 Hz and displacement amplitude of 30 μm were used in all DMA measurements.

Alkaline stability of AAEMs

The alkaline stability of the membranes was monitored by measuring the changes of the ionic conductivity, dimension and IEC values of the membrane before and after being kept in 2.5 M KOH solution at 60 °C. Before being tested the conductivity, dimension and IEC, the membranes were thoroughly washed by deionized water until the conductivity of the water used for washing the membranes was 1.86 μS cm^{-1}.

Single cell tests

The single cell was fabricated by using 70 wt% Pt/C (Johnson Matthey) with metal loading of 0.5 mg cm^{-2} as both anode and cathode catalysts. Quaternized polystyrene polymer was used as the ionomer with a 20% loading at both electrodes. Then the catalyst ink was sprayed onto the AAEMs to obtain catalyst-coated membranes (CCMs). The membrane electrode assemblies (MEAs) were prepared by hot-pressed CCM between two gas diffusion layers (GDLs). The MEA in which the ionmer was in OH form was prepared by immersing the above prepared MEA in 1 M KOH solution at room temperature for 48 h. Before being tested, this MEA was thoroughly washed by deionized water. Cells with 5 cm^2 active area were assembled using stainless steel end-plates. Fuel cell test was carried out with H_2 and O_2 at 50 °C with 100% relative humidity (RH). The flow rates of H_2 and O_2 were 100 and 200 ml min^{-1} with a 0.2 MPa backpressure, respectively. The MEAs were activated by operating at the constant current densities (100, 200 and 300 mA cm^{-2}). After the activation, the fuel cell polarization curve was measured under dynamic current mode. The cell voltage as a function of current density was recorded using fuel cell testing software.

Results and discussion

Conductivities of PEG-grafting SEBS-based AAEMs

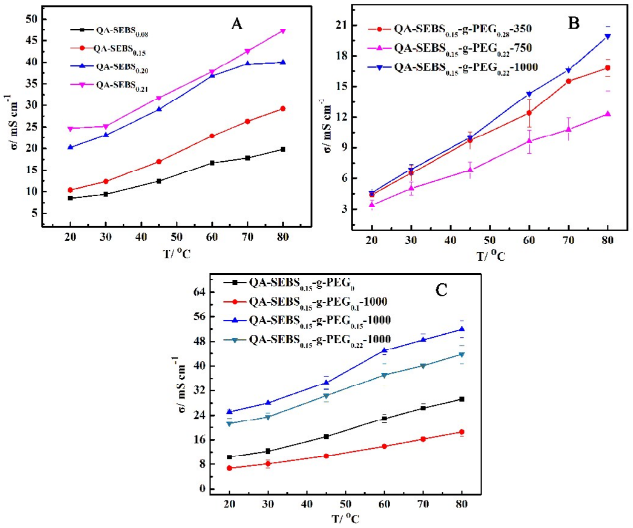

Fig. 2. Conductivities of QA-SEBSx-g-PEGy-M as a function of temperature: A) different CD; B) different molecular weight of PEG; C) different PEG-

grafting degree.

The conductivities of QA-SEBS$_x$-g-PEG$_y$-M would be significantly influenced by the CD of SEBS, the PEG molecular weight and PEG-grafting degree (as shown in Fig. 2). From Fig. 2A, it can be seen that when the CD increases from 0.15 to 0.21, the conductivities of the AAEMs in OH form without PEG-grafting would increase from 10 mS cm^{-1} to 24.7 mS cm^{-1} (room temperature), which is due to the increase of functional degree. To further investigate the influence of the PEG molecular weight and PEG-grafting degree, the CD is fixed at 0.15. By modulating the PEG molecular weight and PEG-grafting degree, the performance of this AAEM is further optimized. From Fig. 2B, it can be seen that the membrane with PEG molecular weight of 1000 shows a higher conductivity than that of the membranes with PEG molecular weight of 350 and 750. Then the properties of the membranes with PEG molecular weight of 1000 were investigated by modulating the PEG-grafting degree. From Fig. 2C, it can be found that the conductivities of the membranes would be significantly influenced by the PEG-grafting degree, increasing from 29.2 mS cm^{-1} to 51.9 mS cm^{-1} at 80 °C when the PEG-grafting degree increases to 0.15, and then decreasing to 43.7 mS cm^{-1} when the PEG-grafting degree is 0.22.

IEC, WU, SD and λ of the membranes

Table 1 shows the IEC, WU, SD, and λ of the QA-SEBS$_{0.15}$-g-PEG$_y$-1000 membranes. The IEC values of the membranes would decrease from 0.75 mmol g^{-1} to 0.42 mmol g^{-1} with the increase of PEG-grafting degree, which is due to the decrease of functional groups and the increase of molecular weight of the polymers. The SD values of these membranes (from 13.5% to 4.2 %) are equal to or even lower than that of the AAEMs with same functional groups (~10%), showing a good dimension stability, especially the QA-SEBS$_{0.15}$-g-PEG$_{0.15}$-1000 membrane. The WU or SD values of SEBS-based AAEMs with or without PEG-grafting were of approximation, indicating that the introduction of PEG didn't evidently change the water-absorption ability and dimension stability of the membranes.

Table 1. IEC, WU, SD and λ of the QA-SEBS0.15-PEGy-1000 membranes (y is 0, 0.1, 0.15 or 0.22).

AAEMs	IEC/ mmol g^{-1}	SD/ %	WU/ %	λ
QA-SEBS0.15-PEG0-1000	0.75	10.3±0.64	5.6±0.1	4.1
QA-SEBS0.15-PEG0.1-1000	0.49	13.5±2.41	4.2±0.5	4.7
QA-SEBS0.15-PEG0.15-1000	0.47	4.2±0.36	4.2±0.7	5.0
QA-SEBS0.15-PEG0.22-1000	0.42	9.9±1.13	3.8±1.1	5.0

From the conductivity and the IEC results of these SEBS-based AAEMs, it can be found that QA-SEBS$_{0.15}$-g-PEG$_{0.15}$-1000 membrane shows relatively lower IEC value but higher conductivity. This result is opposite to the theory law. What factors make the QA-SEBS$_{0.15}$-g-PEG$_{0.15}$-1000 membrane behave the better performance. So to investigate the reason, the micro-phase morphologies of these membranes are investigated deeply by TEM.

Study the effect of the microscale morphology on the physicochemical properties of the membranes

Visually, the prepared membranes are transparent, rather flexible, and can be cut into any sizes or be bent at any degrees. The TEM images of the QA-SEBS$_{0.15}$-g-PEG$_y$-1000 membranes are shown in Fig. 3. The dark strips shown in TEM are the hydrophilic regions of the QA-SEBS$_{0.15}$-g-PEG$_y$-1000 membranes. Using the tri-block copolymer, SEBS, as the main chain, the AAEMs would exhibit a certain of hydrophilic/hydrophobic micro-phase separation structure even if there is no PEG-grafting onto the main chain. Therefore, the morphologies of the AAEMs with or without PEG-grafting wouldn't show any obvious differences from the visual observation. However, the size of hydrophilic-phase is significantly influenced by the PEG-grafting degree. The average sizes of QA-SEBS$_{0.15}$-g-PEG$_0$, QA-SEBS$_{0.15}$-g-PEG$_{0.1}$-1000, QA-SEBS$_{0.15}$-g-PEG$_{0.15}$-1000 and QA-SEBS$_{0.15}$-g-PEG$_{0.22}$-1000 are 8-9nm, 8-9nm, 11-12nm and 15-16nm, respectively. So it can be concluded that the increasing of PEG-grafting onto the SEBS main chain would enlarge the size of ion-conducting channel in the AAEM. The enlarged ion-conducting channel would facilitate the conductivity of OH$^-$, so QA-SEBS$_{0.15}$-g-PEG$_{0.15}$-1000 shows higher conductivity. However, the degradation of IEC, resulted from the larger PEG-grafting degree, would result in the low conductivity, and the conductivity of QA-SEBS$_{0.15}$-g-PEG$_{0.22}$-1000 decreases. Therefore, QA-SEBS$_{0.15}$-g-PEG$_{0.15}$-1000 membrane shows the highest conductivity.

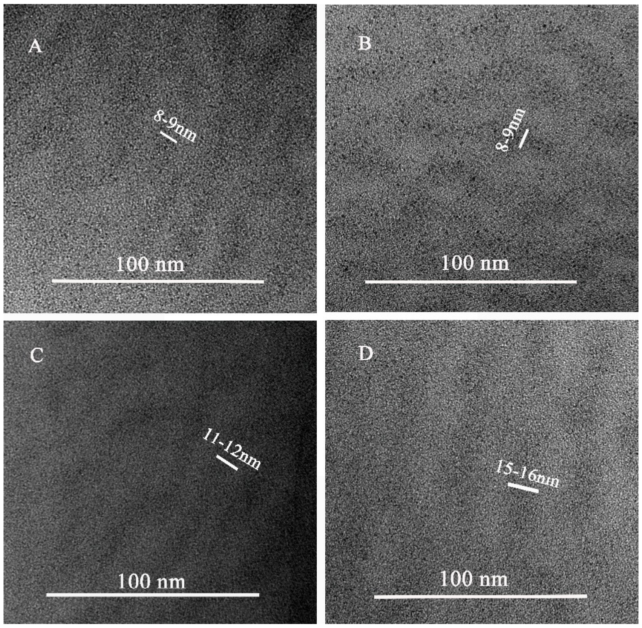

Fig. 3. TEM images of PtCl$_6^{2-}$-stained membranes: (A) QA-SEBS$_{0.15}$-g-PEG$_0$; (B) QA-SEBS$_{0.15}$-g-PEG$_{0.1}$-1000; (C) QA-SEBS$_{0.15}$-g-PEG$_{0.15}$-1000; (D) QA-SEBS$_{0.15}$-g-PEG$_{0.22}$-1000.

Mechanical and thermomechanical stability of the membranes

The SEBS-based AAEMs, which would not be easily broken in the tensile test condition, possessed super mechanical stability, especially the flexible stability at room temperature (as shown in Fig. 4). From Fig. 4, it can be concluded that the tensile strength (15.5 MPa) and elongation at break (250%) values of SEBS-based AAEM are much higher than that of polystyrene-based AAEM (11.5 MPa, 6.2%), indicating the SEBS-based AAEM possesses relatively good toughness and flexibility. Furthermore, the flexibility of the membranes (with elongation at break up to 500% or even not fractured) would be significantly enhanced by grafting PEG onto the SEBS main chain. The dynamic thermomechanical properties of the membranes were investigated by DMA.

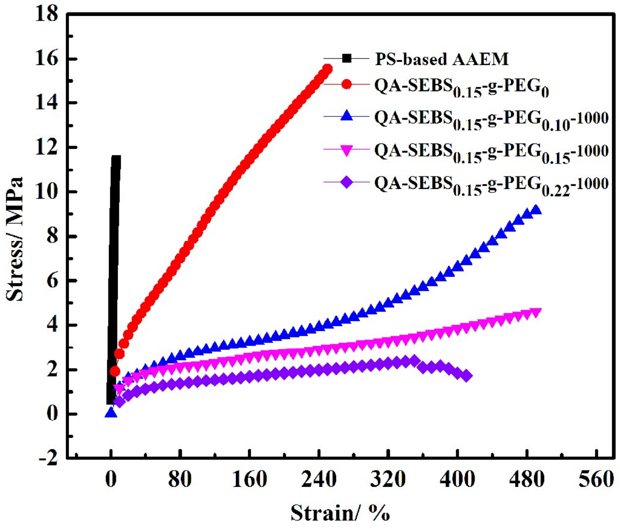

Fig.4. Mechanical stability curves of AAEMs using polystyrene or SEBS as the main chain.

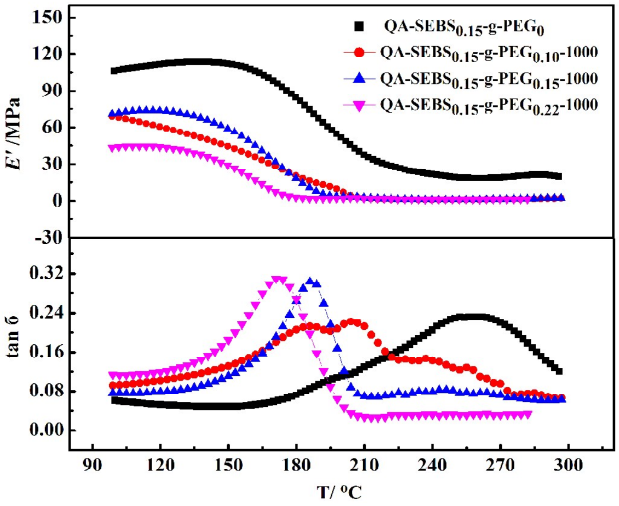

Fig. 5. Storage modulus E' and the damping values Tan δ of QA-SEBS$_{0.15}$-g-PEG$_y$-1000 as a function of temperature.

The storage modulus E' and the damping values Tan δ as a function of temperature are shown in Fig. 5. In general, α-relaxation processes (reflected by the value of Tan δ as a function of temperature) are related to the glass transition temperature, Tg, of the respective membranes. From the DMA test results, it can be seen that PEG-grafting decreases Tg of the membranes (from 258 °C decreases to 170 °C) and the grafting degree wouldn't significantly change Tg of the membranes. Furthermore, Tg of these membranes are all higher than 170 °C. The E' values of these AAEMs would decrease as the PEG grafts onto the SEBS main chain, indicating that the graft of PEG onto the main chain decreases the toughness of the membranes in a certain degree. From the tensile test and DMA test results, it can be concluded that the mechanical strength and thermal performance of these membranes are relatively good, which could meet the requirement of the alkaline electrochemical system working condition (<100 °C), showing an application potential in the electrochemical systems, eg. fuel cells.

Alkaline stability of AAEMs

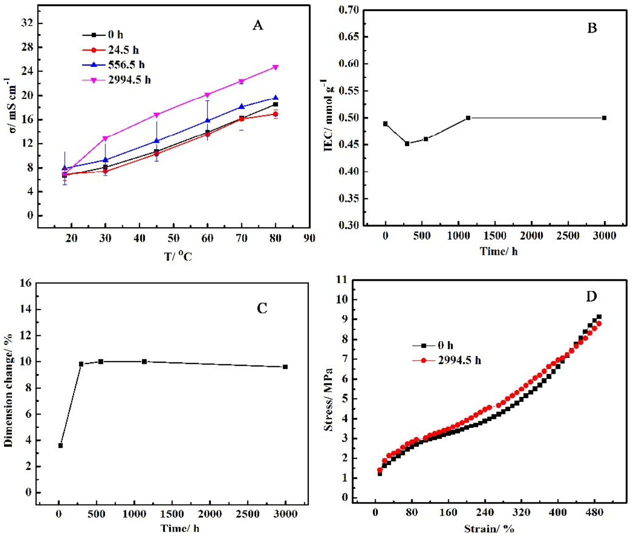

Fig. 6. Changes of conductivity, IEC, dimension and mechanical property of QA-SEBS$_{0.15}$-g-PEG$_{0.1}$-1000 after the exposure to 2.5 M KOH at 60 °C for different time.

Alkaline stability of the AAEMs is a vital property to evaluate the potential application of AAEMs in the severe alkaline environment. Though it has been proved that the OH- concentration of 1 M was enough to be used to ex-situ elevate the alkaline stability of AAEMs for the application of fuel cells[23, 26, 32], it is still necessary to further determine the alkaline stability of the AAEMs in the severe alkaline condition. Therefore, higher concentration alkaline solution (2.5 M KOH) is used in this work to investigate the alkaline stability of the QA-SEBS$_x$-g-PEG$_y$-M. The changes of ion conductivity, IEC, in-plane dimension and mechanical property of the membranes before and after being treated in 2.5 KOH at 60 °C are used to estimate the alkaline stability of these AAEMs. From Fig. S2 and Fig. 6, it can be found that the conductivity, IEC and mechanical property values of PEG-grafting membrane would remain almost unchangeable in 1 M and 2.5 M KOH (this concentration is rarely used in the references to confirm the alkaline stability of AAEMs) at 60 °C.

This AAEM would swell in 2.5 M KOH at 60 °C for 300 h and then remain stable in this environment. From the test results, it can be concluded that the main chain and the functional group of the QA-SEBSx-g-PEGy-M AAEMs are stable enough in 2.5 M KOH at 60 °C for about 3000 h, which is equal to even better than that of the other AAEMs in the references[15, 29, 33] (Table S1).

Performance of the fuel cell using SEBS-based AAEM

The SEBS-based AAEMs show very good physicochemical properties, such as high conductivity, mechanical and chemical stability, so the QA-SEBS$_{0.2}$-g-PEG$_0$-M membrane is used to fabricate the membrane electrode assembly (MEA). Fig. 7 showed the polarization and power density curves of the alkaline anion exchange membrane fuel cell (AAEMFC) at 50 °C using the above MEAs. From Fig. 7, it can be seen that the open-circuit voltage and the peak power density of the fuel cell are over 1.04 V and 146 mW cm^{-2}, indicating that QA-SEBS$_{0.2}$-g-PEG$_0$-M possesses relatively good gas-separation ability and ion-conductivity property.

It should be also noted that the performance of the fuel cell using SEBS-based membranes could be improved by further optimizing the electrode structure and lowering the resistance of the membranes.

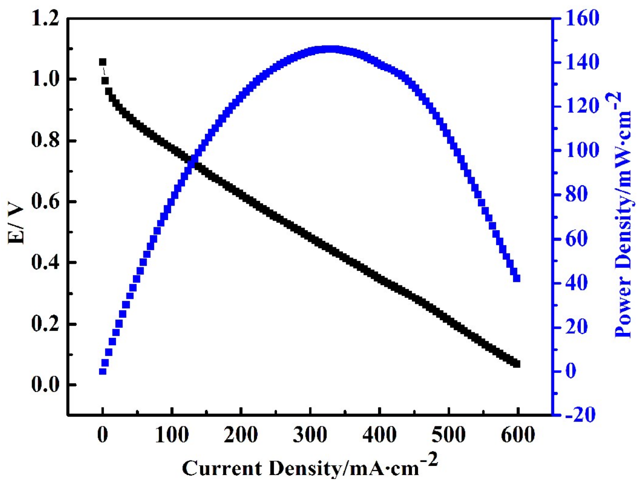

Fig. 7. Polarization and power density curves of AAEMFCs assembled using QA-SEBS$_{0.2}$ as AAEMs. The test temperature was 50 °C.

4. Conclusions

The PEG-grafting SEBS-based AAEMs with highly mechanical and chemical stability and conductivity were designed, prepared and characterized. The elongation at break of SEBS-based AAEMs is 80 times over that of the polystyrene-based membranes. Remarkably, these AAEMs could be stable enough in 2.5 M KOH at 60 °C for about 3000 h, which is rare in the recent study results. Furthermore, the properties of the membranes could be optimized by modulating the CD of SEBS, PEG molecular weight or the PEG-grafting degree. Especially, the graft of the PEG could enhance the conductivity of these AAEMs (80 °C, from 29.2 mS cm^{-1} to 51.9 mS cm^{-1}) due to the enlargement of the ion-conducting channel (revealed by TEM). The peak power density of H_2/O_2 single fuel cell using this SEBS-based AAEM is up to 146 mW cm^{-2} at 50 °C.

However, there is still a query on the relationship between the conductivity of AAEM and the size of ion-conducting channel. The size of the hydrated OH$^-$ is not clear until now, thus it is disputed that what size of the channel is most favorable for the conduction of OH$^-$ in AAEM. It is necessary to adequately understand the influence of the microscale structure (especially the size of the ion-conducting channel) on the property of AAEM, which is more important for enhancing the property of AAEM by designing the microscale-structure.

Acknowledgement

This work is financially supported by the National Basic Research Program of China (2012CB215500).

Notes and references

[a] *Division of Fuel Cell & Battery, Dalian National Laboratory for Clean Energy, Dalian Institute of Chemical Physics, Chinese Academy of Sciences, 457 Zhongshan Road, Dalian 116023, PR China*。gqsun@dicp.ac.cn; *Tel: +86-411-84379063*
[b] *University of the Chinese Academy of Sciences, Beijing 100039, PR China*
[c] *Dalian University of Technology, Dalian 116023, PR China.*

† Electronic Supplementary Information (ESI) available: ^{1}H NMR spectra of SEBS, CMSEBS and SEBSx-g-PEGy-M, alkaline Stability of QA-SEBS0.15-G-PEGy-1000, some explanation for the performance of the fuel cell using SEBS-based AAEM. See DOI: 10.1039/b000000x/

1. J. Pan, C. Chen, L. Zhuang and J. Lu, *Accounts of Chemical Research*, 2011, **45**, 473-481.
2. J. Pan, Y. Li, J. Han, G. Li, L. Tan, C. Chen, J. Lu and L. Zhuang, *Energy & Environmental Science*, 2013, **6**, 2912-2915.
3. N. Li, M. D. Guiver and W. H. Binder, *ChemSusChem*, 2013, **6**, 1376-1383.
4. B. Schwenzer, J. Zhang, S. Kim, L. Li, J. Liu and Z. Yang, *ChemSusChem*, 2011, **4**, 1388-1406.
5. S. L. Mallinson, J. R. Varcoe and R. C. T. Slade, *Electrochimica Acta*, 2014, **140**, 145-151.
6. P. G. Bruce, S. A. Freunberger, L. J. Hardwick and J.-M. Tarascon, *Nat Mater*, 2012, **11**, 19-29.
7. D. Pletcher and X. Li, *International Journal of Hydrogen Energy*, 2011, **36**, 15089-15104.
8. Y. Leng, G. Chen, A. J. Mendoza, T. B. Tighe, M. A. Hickner and C.-Y. Wang, *Journal of the American Chemical Society*, 2012, **134**, 9054-9057.
9. E. Guler, Y. Zhang, M. Saakes and K. Nijmeijer, *ChemSusChem*, 2012, **5**, 2262-2270.
10. H. Luo, P. Xu, P. E. Jenkins and Z. Ren, *Journal of Membrane Science*, 2012, **409–410**, 16-23.
11. J. Ran, L. Wu, Q. Ge, Y. Chen and T. Xu, *Journal of Membrane Science*, 2014, **470**, 229-236.
12. J. Pan, C. Chen, Y. Li, L. Wang, L. Tan, G. Li, X. Tang, L. Xiao, J. Lu and L. Zhuang, *Energy & Environmental Science*, 2014, **7**, 354-360.
13. J. R. Varcoe, P. Atanassov, D. R. Dekel, A. M. Herring, M. A. Hickner, P. A. Kohl, A. R. Kucernak, W. E. Mustain, K. Nijmeijer, K. Scott, T. Xu and L. Zhuang, *Energy & Environmental Science*, 2014, **7**, 3135-3191.
14. B. Lin, H. Dong, Y. Li, Z. Si, F. Gu and F. Yan, *Chemistry of Materials*, 2013, **25**, 1858-1867.
15. J. Han, Q. Liu, X. Li, J. Pan, L. Wei, Y. Wu, H. Peng, Y. Wang, G. Li, C. Chen, L. Xiao, J. Lu and L. Zhuang, *ACS Applied Materials & Interfaces*, 2015, **7**, 2809-2816.
16. X. Wang, M. Li, B. T. Golding, M. Sadeghi, Y. Cao, E. H. Yu and K. Scott, *International Journal of Hydrogen Energy*, 2011, **36**, 10022-10026.

17. G. Merle, M. Wessling and K. Nijmeijer, *Journal of Membrane Science*, 2011, **377**, 1-35.
18. O. M. M. Page, S. D. Poynton, S. Murphy, A. Lien Ong, D. M. Hillman, C. A. Hancock, M. G. Hale, D. C. Apperley and J. R. Varcoe, *RSC Advances*, 2013, **3**, 579-587.
19. Z. Si, L. Qiu, H. Dong, F. Gu, Y. Li and F. Yan, *ACS Applied Materials & Interfaces*, 2014, **6**, 4346-4355.
20. O. D. Thomas, K. J. W. Y. Soo, T. J. Peckham, M. P. Kulkarni and S. Holdcroft, *Journal of the American Chemical Society*, 2012, **134**, 10753-10756.
21. W. Li, S. Wang, X. Zhang, W. Wang, X. Xie and P. Pei, *International Journal of Hydrogen Energy*, 2014, **39,** 13710-13717.
22. K. J. T. Noonan, K. M. Hugar, H. A. Kostalik, E. B. Lobkovsky, H. D. Abruña and G. W. Coates, *Journal of the American Chemical Society*, 2012, **134**, 18161-18164.
23. Y. Zha, M. L. Disabb-Miller, Z. D. Johnson, M. A. Hickner and G. N. Tew, *Journal of the American Chemical Society*, 2012, **134**, 4493-4496.
24. S. Chempath, J. M. Boncella, L. R. Pratt, N. Henson and B. S. Pivovar, *The Journal of Physical Chemistry C*, 2010, **114**, 11977-11983.
25. F. Gu, H. Dong, Y. Li, Z. Si and F. Yan, *Macromolecules*, 2013, **47**, 208-216.
26. C. Yang, S. Wang, W. Ma, L. Jiang and G. Sun, *Journal of Membrane Science,* 2015, **487**, 12–18.
27. S. A. Nuñez and M. A. Hickner, *ACS Macro Letters*, 2012, **2**, 49-52.
28. O. I. Deavin, S. Murphy, A. L. Ong, S. D. Poynton, R. Zeng, H. Herman and J. R. Varcoe, *Energy & Environmental Science*, 2012, **5**, 8584-8597.
29. N. Li, Y. Leng, M. A. Hickner and C.-Y. Wang, *Journal of the American Chemical Society*, 2013, **135**, 10124-10133.
30. C. G. Arges and V. Ramani, *Proceedings of the National Academy of Sciences*, 2013, **110**, 2490-2495.
31. C. G. Arges and V. Ramani, *Journal of The Electrochemical Society*, 2013, **160**, F1006-F1021.
32. C. Yang, S. Wang, W. Ma, L. Jiang and G. Sun, *Journal of Materials Chemistry A*, 2015, **3**, 8559-8565.
33. J. Ran, L. Wu, B. Wei, Y. Chen and T. Xu, *Sci. Rep.*, 2014, **4**.